CrystEngComm

Cite this: *CrystEngComm*, 2011, **13**, 2890

www.rsc.org/crystengcomm

PAPER

Metallomacrocycle or coordination polymer: Spacer-directed self-assembly of transition-metal complexes based on flexible bis(benzotriazole) ligands†

Xiao-Liang Tang, Wei Dou, Ji-an Zhou, Guo-Lin Zhang, Wei-Sheng Liu,* Li-Zi Yang and Yong-Liang Shao

Received 12th November 2010, Accepted 26th January 2011
DOI: 10.1039/c0ce00847h

Three structurally related flexible bis(benzotriazole) ligands, 1,2-bis(benzotriazol-1-yl)ethane ($\mathbf{L^1}$), 1,5-bis(benzotriazol-1-yl)-3-oxapentane ($\mathbf{L^2}$) and 1,8-bis(benzotriazol-1-yl)-3,6-dioxaoctane ($\mathbf{L^3}$), have been synthesized. They were reacted with $AgNO_3$ and $CuCl_2 \cdot 2H_2O$ at room temperature, resulting in the formation of six novel complexes: $\{[Ag\mathbf{L^1}(NO_3)(CH_3CN)]\}_n$ (**1**), $[Ag_2(\mathbf{L^2})_3](NO_3)_2$ (**2**), $\{[Ag_2(\mathbf{L^3})_2(NO_3)_2]\}_n$ (**3**), $\{[Cu\mathbf{L^1}Cl_2]\}_n$ (**4**), $[Cu_2(\mathbf{L^2})_2Cl_4]$ (**5**), and $[Cu_2(\mathbf{L^3})_2Cl_4(DMF)_2]$ (**6**). All complexes have been characterized by X-ray diffraction analysis. In **1** and **4**, they exhibit similar coordination modes in which each ligand links two metal ions to form a 1D non-linear coordination polymeric chain. In **2**, two Ag^I centers are close coupled by Ag···Ag interaction and three bridging ligands to form a dinuclear cation. The structure of **3** reveals the dinuclear cluster units, formed by two ligands and two Ag^I ions, are linked by anions to self-assemble a 1D chain. Complex **5** is an isolated dinuclear structure, in which ligands and bridging chloro ligands act as the organic clips to bridge two Cu^{II} centres. But in **6**, a pair of ligands takes on the conformation to connect two metal ions to form bimetallic a macrocyclic architecture. These results unequivocally indicate that the influence of flexible ligand spacers, which bring structural varieties for the same metal ion, is the key factor governing the molecular architectures. Moreover, the thermal stability of **1–3** and **4–6** in the solid state has also been compared.

Introduction

One of the major goals of crystal engineering is targeted at the predictable assembly of molecular species.[1] Considerable effort has been devoted to understanding the self-assembly of organic and inorganic molecules in the past decade because it extends the range of new solids that can be designed to have particular physical and chemical properties.[2] Generally speaking, the generation of self-assembling coordination architectures depends on the combination of several factors, such as the coordination geometry of the metal ions, the performance of the ligands, the coordinated and/or non-coordinated counter ions, the solvent systems and the reaction conditions.[3] The ligand is no doubt the key factor for manipulating the structures of the complexes. Therefore, the application of a special metal ion and the use of a well-designed ligand to control the assembly of molecular architectures have become a popular and rapidly growing discipline.[4]

Up to now, most coordination architectures have been widely constructed by Yaghi, Williams, Férey, Chen, Hong and their co-workers with rigid linear bridging ligands, such as 1,4-benzenedicarboxylic acid, 1,3,5-benzenetricarboxylic acid, pyrazine and 4,4′-bipyridine.[5] More recently, increasing attention has been paid to employ flexible ligands for several reasons: (a) such ligands possess stronger capability in coordination by prolonging their arms and weakening stereo-hindrance effects; (b) they can adopt various conformations and gain access to novel supramolecular structures not available from the logical combination of rigid building blocks;[6] (c) the incorporation of flexible components may endow the molecular architectures with potential advantages, for example, a "breathing" ability in the solid state and adaptive recognition properties.[7] Nevertheless, due to the structural flexibility and conformational freedoms of such ligands, rational design and precise control of the final product supramolecular architectures from 0D to 3D are still great challenges to chemists.[3,8]

Benzotriazole has been extensively used as a synthetic auxiliary in organic chemistry and a corrosion inhibitor in materials science.[9] An important part within its application is to obtain the deprotonated benzotriazolate anion, which can

Key Laboratory of Nonferrous Metals Chemistry and Resources Utilization of Gansu Province and State Key Laboratory of Applied Organic Chemistry, College of Chemistry and Chemical Engineering, Lanzhou University, Lanzhou, 730000, China. E-mail: liuws@lzu.edu.cn; Fax: +86-931-8912582; Tel: +86-931-8915151

† Electronic supplementary information (ESI) available: The characterization IR of the ligands; IR, the tables of hydrogen bonds, π–π interactions, selected bond lengths and selected bond angles of the complexes **1–6**. CCDC reference numbers 676484–676489. For ESI and crystallographic data in CIF or other electronic format see DOI: 10.1039/c0ce00847h

coordinate up to three metal centres *via* its three nitrogen donors.[10] Until recently, some substituted benzotriazoles with rigid moieties have been investigated in supramolecular coordination chemistry because more intermolecular interactions such as hydrogen bonds and π–π stacking interactions are often observed in solid structures.[11] However, there are relatively few systematic studies on flexible benzotriazole ligands with different spacers and their complexes with various structural features.

We are engaging in a detailed study on the influence of metal ions, various terminal groups, and open-chain crown ether spaces on the coordination supramolecular structures.[12] In this work, our idea is to introduce benzotriazoles into a flexible oligoethyleneglycol skeleton with different length spacers to further explore the relationship between flexible chain and low-dimensional (0D or 1D) structural features. Therefore, we designed three structurally related flexible ligands: 1,2-bis(benzotriazol-1-yl)ethane (**L¹**), 1,5-bis(benzotriazol-1-yl)-3-oxapentane (**L²**) and 1,8-bis(benzotriazol-1-yl)-3,6-dioxaoctane (**L³**) (Scheme 1), and obtained correlative crystal structures of six novel complexes, $\{[AgL^1(NO_3)(CH_3CN)]\}_n$ (**1**), $[Ag_2(L^2)_3](NO_3)_2$ (**2**), $\{[Ag_2(L^3)_2(NO_3)_2]\}_n$ (**3**), $\{[CuL^1Cl_2]\}_n$ (**4**), $[Cu_2(L^2)_2Cl_4]$ (**5**), and $[Cu_2(L^3)_2Cl_4(DMF)_2]$ (**6**). The structure formations of the six compounds are presented and their thermogravimetric analyses are discussed.

Experimental section

Materials and methods

All the reagents used for the syntheses of **1–6** were commercially available and employed without further purification or purified by standard methods prior to use. Elemental analyses were performed on a Vario EL elemental analyzer. IR spectra were recorded on a Nicolet Avatar 360 FT-IR instrument using KBr discs in the 400–4000 cm^{-1} region. ^1H NMR spectra were recorded on a Varian Mercury plus 300BB spectrometer at 25 °C in $CDCl_3$ with tetramethylsilane as the internal reference. Thermogravimetric and differential thermal analysis (TG-DTA) experiments were performed on a Perkin-Elmer TG/DTA-6300 instrument from room temperature to 750 °C under a nitrogen atmosphere at a heating rate of 10 °C min^{-1}.

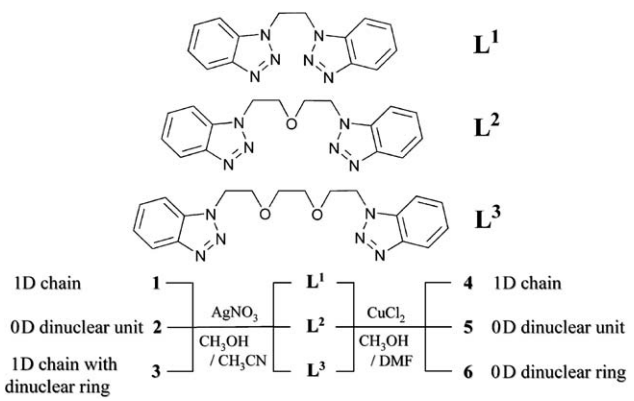

Scheme 1 Structures of the ligands, **L¹–L³**, and schematic view of the syntheses of the six complexes **1–6**.

Synthesis of ligands

The three ligands were prepared by the adoption of a similar reported procedure.[11e] The reactions of benzotriazole with 1,2-bis(*p*-tolylsulfonyloxy)ethane, 1,5-bis(*p*-tolylsulfonyloxy)-3-oxapentane or 1,8-bis(*p*-tolylsulfonyloxy)-3,6-dioxaoctane in the presence of sodium hydroxide in absolute methanol, under reflux conditions over 6 h, gave a mixture of isomers. The solvent was evaporated and the mixture was taken up in $CHCl_3$ and washed at least three times with H_2O before being dried over anhydrous $MgSO_4$. **L¹**, **L²** and **L³** were further separated by column chromatography on silica gel, and the white product was characterized by ^1H NMR and IR spectra.

For **L¹**, yield: 28.4%; m.p. 157.6–158.9 °C. ^1H NMR ($CDCl_3$, ppm): δ 5.25 (s, 4H), 6.83∼6.88 (d, 2H), 7.14∼7.21 (m, 4H), 7.86∼7.91 (d, 2H). IR (cm^{-1}, KBr): 3066w, 1608w, 1493m, 1449m, 1306m, 1277m, 1218s, 1157m, 1125w, 1055vs, 996w, 789m, 752vs.

For **L²**, yield: 32.8%; m.p. 76.4–77.3 °C. ^1H NMR ($CDCl_3$, ppm): δ 3.90∼3.95 (t, 4H), 4.67∼4.71 (t, 4H), 7.32∼7.39 (m, 6H), 8.00∼8.05 (d, 2H). IR (cm^{-1}, KBr): 3058m, 2959w, 1615w, 1495w, 1455m, 1308w, 1269m, 1227s, 1159s, 1114s, 1033m, 975m, 860w, 775m, 739vs.

For **L³**, yield: 34.1%; m.p. 91.5–92.6 °C. ^1H NMR ($CDCl_3$, ppm): δ 3.39 (s, 4H), 3.79∼3.83 (t, 4H), 4.67∼4.71 (t, 4H), 7.32∼7.38 (t, 2H), 7.41∼7.47 (t, 2H), 7.51∼7.54 (d, 2H), 8.01∼8.05 (d, 2H). IR (cm^{-1}, KBr): 3067w, 2899s, 2876m, 1615w, 1495m, 1458m, 1402w, 1358w, 1328m, 1266w, 1230s, 1124vs, 1020s, 779m, 750s

Preparation of complexes 1–6

$\{[AgL^1(NO_3)(CH_3CN)]\}_n$ (1). The reaction of **L¹** (26.4 mg, 0.1 mmol) with $AgNO_3$ (17.0 mg, 0.1 mmol) in methanol (10 mL) for a few minutes afforded a white solid, which was filtered, washed with methanol, and dried in vacuum. Colorless block single crystals suitable for X-ray analysis were obtained by slow evaporation of methanol and acetonitrile mixed solution (V : V = 5 : 1) of the complex at room temperature in the dark. Yield: 64%. Anal. Calcd for $C_{16}H_{15}AgN_8O_3$: C, 40.44; H, 3.18; N, 23.58. Found: C, 40.61; H, 2.77; N, 23.65. IR (KBr, cm^{-1}): 3463w, 3064w, 1610w, 1495w, 1453m, 1385vs, 1307m, 1217s, 1157m, 1108w, 1055s, 997w, 751vs.

$[Ag_2(L^2)_3](NO_3)_2$ (2). Colorless block single crystals for X-ray analysis were obtained by similar method as described for **1**. Yield: 70%. Anal. Calcd for $C_{48}H_{48}Ag_2N_{20}O_9$: C, 45.58; H, 3.83; N,22.15. Found: C, 45.66; H, 3.52; N, 22.31. IR (KBr, cm^{-1}): 3427w, 3062w, 2873w, 1614w, 1495w, 1454m, 1368vs, 1271m, 1230s, 1161m, 1121s, 1036m, 749vs.

$\{[Ag_2(L^3)_2(NO_3)_2]\}_n$ (3). Colorless block single crystals for X-ray analysis were obtained by similar method as described for **1**. Yield: 51%. Anal. Calcd for $C_{18}H_{20}AgN_7O_5$: C, 41.40; H, 3.86; N, 18.77. Found: C, 41.61; H, 3.39; N, 18.42. IR (KBr, cm^{-1}): 3444w, 2950w, 2920w, 2859w, 1495w, 1458m, 1415vs, 1282vs, 1229s, 1171m, 1132s, 1108s, 1041m, 1025m, 894m, 747s, 713m, 668w.

{[CuL^{1}Cl$_2$]}$_n$ (4). The reaction of **L^1** (26.4 mg, 0.1 mmol) with $CuCl_2 \cdot 2H_2O$ (17.1 mg, 0.1 mmol) in methanol (10 mL) for a few minutes afforded a navy blue solid, which was filtered, washed with methanol, and dried in vacuum. Navy blue block single crystals suitable for X-ray analysis were obtained by slow evaporation of methanol and DMF mixed solution (V : V = 10 : 1) of the complex at room temperature. Yield: 45%. Anal. Calcd for $C_{14}H_{12}Cl_2CuN_6$: C, 42.17; H, 3.03; N, 21.08. Found: C, 42.20; H, 2.63; N, 21.34. IR (KBr, cm^{-1}): 3433w, 3061w, 2952w, 1592w, 1493w, 1440m, 1359w, 1292m, 1234s, 1187s, 1165m, 1124m, 964w, 772s, 747vs.

[Cu$_2$(L^2)$_2$Cl$_4$] (5). Green block single crystals were obtained by similar method as described for **4**. Yield: 55%. Anal. Calcd for $C_{32}H_{32}Cl_4Cu_2N_{12}O_2$: C, 43.40; H, 3.64; N, 18.98. Found: C, 43.35; H, 3.80; N, 19.12. IR (KBr, cm^{-1}): 3445w, 3038w, 2958w, 2912w, 2875w, 1591w, 1482w, 1451m, 1354w, 1324w, 1285m, 1234m, 1190m, 1129s, 1045w, 916w, 750vs.

[Cu$_2$(L^3)$_2$Cl$_4$(DMF)$_2$] (6). Green block single crystals were obtained by similar method as described for **4**. Yield: 46%. Anal. Calcd for $C_{42}H_{54}Cl_4Cu_2N_{14}O_6$: C, 45.05; H, 4.86; N, 17.51. Found: C, 45.21; H, 4.39; N, 17.74. IR (KBr, cm^{-1}): 3427w, 2925w, 2865w, 1652vs, 1446w, 1383m, 1330m, 1234m, 1183w, 1134m, 1106m, 1061m, 1033w, 914w, 741s, 668w.

X-ray data collection and structure determination

Single-crystal X-ray diffraction measurements were carried out on a Bruker Smart APEX II or 1000 CCD diffractometer equipped with a graphite crystal monochromator situated in the incident beam for data collection at room temperature. The determination of unit cell parameters and data collections was performed with Mo-Kα radiation (λ = 0.71073 Å). Multi-scan absorption correction was applied with the SADABS program.[13] Unit cell dimensions were obtained with least-squares refinements, and all structures were solved by direct methods using SHELXS-97.[14] Metal atoms in each complex were located from E-maps. The non-hydrogen atoms were located in successive difference Fourier syntheses (in complex **2**, the oxygen atoms of the nitrate anions are disordered and treated isotropically). The final refinement was performed by full matrix least-squares methods with anisotropic thermal parameters for non-hydrogen atoms on F^2. The hydrogen atoms were introduced at calculated positions and not refined (riding model). The details of the crystal parameters, data collections and refinement for **1–6** are summarized in Table 1. Selected bond lengths, with the estimated standard deviations, hydrogen bonds and π–π interactions in the crystals are listed in Tables S1–S6 (ESI†).

Results and discussion

The construction of supramolecular structures is highly influenced by several factors, such as the geometric preference of metal ions, the size and shapes of the organic building blocks, the metal–ligand ratio, templates, the solvent systems and the counter-ions. Therefore, it is necessary to decrease various different disturbance factors as much as possible to explore the contributions of ligands, especially flexible spacers, on complex structures. The metal ions of subgroup elements Cu and Ag were chosen as central ions of metal complexes, and both of them belong to the family IB of the periodic table but only have a different number of electrons in their outermost *d* orbital. For Ag complexes **1**, **2** and **3**, they were assembled under the same conditions except for the ligand structure, which made the study on the effect of the ligand relatively accurate. When Cu^{II} was used instead of Ag^I, complexes **4**, **5** and **6**, with different supramolecular structures, were achieved under the same crystal growth environment (Scheme 1).

Structural investigations in the crystalline phase

Crystal structure of complex 1. Crystals of **1** belong to a centrosymmetric space group $P\bar{1}$. The asymmetric unit contains one ligand **L^1**, one nitrate anion and one CH_3CN molecule—all coordinated to the metal center Ag^I. As shown in Fig. 1a, the Ag^I center adopts a distorted tetrahedron coordination consisting of two benzotriazole N-donors, an O-donor from the nitrate anion and a N-donor from the CH_3CN molecule with a long Ag–N bond length [Ag(1)–N(8) = 2.553(4) Å]. In this structure, **L^1** displays a folded V-shape and two N coordination sites in benzotriazole groups point outwards in the opposite direction to make **L^1** form a *trans*-conformation bridging ligand. The dihedral angle of two benzotriazole planes is 37.77°. Coordination of the V-shaped ligand with the adjacent metal centers leads to the formation of a 1D non-linear coordination polymeric chains along the crystallographic *b* axis, which are further self-assembled in an *anti*-parallel fashion and arranged alternately in the solid state *via* two sets of interchain π–π interactions between the benzotriazole–benzotriazole groups (Fig. 1b). The corresponding face-to-face minimum distances are 3.54 and 3.68 Å, respectively. Moreover, these 1D non-linear coordination polymeric chains are further held together by weak C–H···O and C–H···N hydrogen bonds [C(8)···O(1) = 3.307(5) Å, C(8)···O(3) = 3.292(5) Å and C(15)···N(5) = 3.353(6) Å], and the supramolecular architecture is stabilized.

Crystal structure of complex 2. The structure of complex **2** is crystallized in the trigonal space group $R\bar{3}c$, with each unit cell containing six independent $[Ag_2(\mathbf{L^2})_3]^{2+}$ cations. The complex has D_3 symmetry, and Fig. 2a clearly shows a three-dimensional view of the dinuclear $[Ag_2(\mathbf{L^2})_3]^{2+}$ cation, viewed approximately along the threefold axis, whose direction is the same as the crystallographic *c* axis. In the dinuclear unit of complex **2**, two Ag^I centers are close coupled *via* an Ag···Ag interaction along the threefold axis, and the distance between them is 3.186(1) Å. The two metal centres are further bridged by three ligands each of which coordinates to the silver atom in a monodentate mode *via* the N(1) of the benzotriazole ring. The triangle coordination geometry of the silver atom is equilateral, with the N–Ag–N angle being 120°. As shown in Fig. 2b, three benzotriazole rings attaching to the Ag^I center are all lying approximately co-planar, although there are slight deviations from the idealistic coordination plane consisting of three N(1) atoms. The dihedral angle between the benzotriazole ring plane and the coordination plane is *ca.* 6.53°. On the other hand, the two coordination planes in the dinuclear cation are further linked through a set of π–π interactions between phenyl–phenyl groups, with the distances

Table 1 Crystallographic data and structure refinement summary for **1–6**

Complex	**1**	**2**	**3**	**4**	**5**	**6**
Chemical formula	$C_{16}H_{15}AgN_8O_3$	$C_{48}H_{48}Ag_2N_{20}O_9$	$C_{18}H_{20}AgN_7O_5$	$C_{14}H_{12}Cl_2CuN_6$	$C_{32}H_{32}Cl_4Cu_2N_{12}O_2$	$C_{42}H_{54}Cl_4Cu_2N_{14}O_6$
Formula weight	475.23	1264.80	522.28	398.74	885.58	1119.87
Crystal system	Triclinic	Rhombohedral	Monoclinic	Triclinic	Triclinic	Orthorhombic
Space group	$P\bar{1}$	$R\bar{3}c$	$P2_1/c$	$P\bar{1}$	$P\bar{1}$	$Pbca$
a/Å	9.7616(13)	15.282(2)	11.302(4)	7.7004(14)	8.7198(7)	35.704(6)
b/Å	9.9673(13)	15.282(2)	9.866(3)	9.5195(18)	10.1265(9)	33.360(5)
c/Å	11.530(3)	40.377(4)	19.300(5)	11.112(2)	10.9772(9)	8.2196(13)
α/°	104.062(3)	90.00	90.00	79.404(3)	88.4220(10)	90.00
β/°	99.128(3)	90.00	107.972(15)	86.652(3)	73.7320(10)	90.00
γ/°	115.917(2)	120.00	90.00	80.058(3)	72.3070(10)	90.00
V/Å^3	932.6(3)	8166.3(17)	2047.1(11)	788.3(3)	884.72(13)	9790(3)
T/K	294(2)	293(2)	294(2)	294(2)	294(2)	294(2)
Z	2	6	4	2	1	8
D_c/g cm^{-3}	1.692	1.543	1.695	1.680	1.662	1.520
μ/mm^{-1}	1.117	0.792	1.032	1.731	1.555	1.149
F(000)	476	3852	1056	402	450	4624
Refl. measured	4777	11 063	11 391	3987	4525	55 832
Unique refl. (R_{int})	3329 (0.0182)	1545 (0.0327)	4367 (0.0236)	2765 (0.0236)	3149 (0.0140)	11 128 (0.1315)
GOF on F^2	1.004	1.013	1.034	1.031	1.016	1.012
R_1 [$I > 2\sigma(I)$][a]	0.0318	0.0704	0.0290	0.0453	0.0310	0.0916
wR_2 [$I > 2\sigma(I)$][b]	0.0755	0.1886	0.0716	0.1075	0.0703	0.1546

[a] $R_1 = \Sigma||F_o| - |F_c||/|F_o|$. [b] $wR_2 = \{\Sigma[w(F_o^2 - F_c^2)]^2/\Sigma[w(F_o^2)]^2\}^{1/2}$.

between phenyl ring centroids all being 3.66 Å. As counterions, two non-coordinated nitrate groups are disordered over two orientations and are located near the dinuclear cation. In addition, as displayed in Fig. 2c, the spacious dinuclear cations are effectively connected by these nitrate counterions *via* the weak hydrogen bonds C–H···O [C(6)···O(2) = 3.219(10) Å, C(7)···O(2) = 3.214(9) Å and C(8)···O(2) = 2.947(13) Å], accompanied with parallel π–π interactions between the dinuclear cations, to form the three-dimensional stacking.

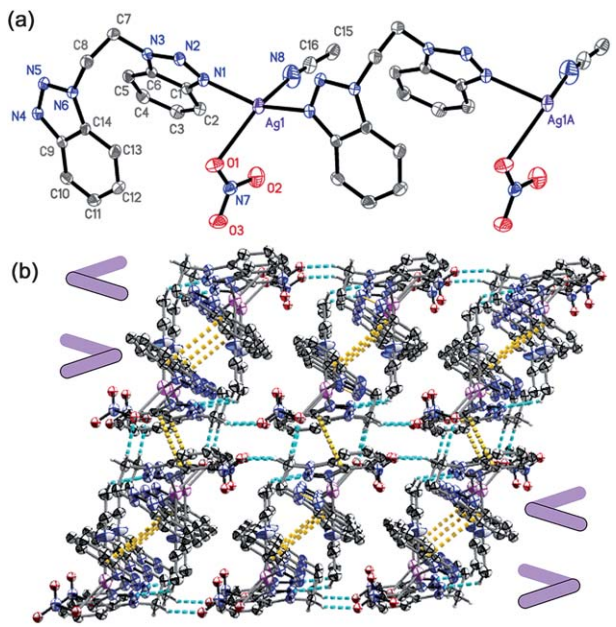

Fig. 1 (a) ORTEP drawing showing the molecular structure of **1** (30% probability ellipsoids). Hydrogen atoms are omitted for clarity. Symmetry code: (A) x, $-1 + y$, z. (b) Aggregations of alternate 1D chains link each other through a series of hydrogen bonds and π–π stacking interactions. Hydrogen bonds are denoted by the turquoise broken line; π–π stacking interactions are indicated by the orange broken line. The lavender symbol represents 1D non-linear chains, constructed by a V-shaped ligand in an *anti*-parallel fashion, to arrange alternately in the solid state.

Crystal structure of complex 3. Complex **3** is a one-dimensional polymeric chain comprised of the neutral $[Ag_2(\mathbf{L^3})_2(NO_3)_2]$ as the repeating unit (Fig. 3a). Each Ag^I center is bonded to two N donors of two benzotriazole rings from two distinct $\mathbf{L^3}$ ligands and two O donors from two nitrate anions. The coordination geometry can be described as a distorted tetrahedron. In the polymeric structure, two species of rings with different sizes are assembled and linked alternately by Ag^I ions. One of them is a centrosymmetric 30-membered macrometallacycle formed by two $\mathbf{L^3}$ ligands bridging two Ag^I ions. The Ag···Ag non-bonding distance in the dinuclear unit is 8.241 Å, and the two terminal benzotriazole rings in the same ligand have a dihedral angle of *ca.* 63.68°. In addition, it is shown that the cavity encircled by the macrometallacycle is S-shaped and there are no molecules filling it in. The other ring species are also centrosymmetric, with two oxygen atoms from two nitrate groups bridging the two silver atoms to obtain an obligate-planar 4-membered Ag(μ–O)$_2$Ag ring. The distance of Ag···Ag is 3.953 Å. As indicated in Fig. 3b, there are a series of weak C–H···O hydrogen bonds [C(14)···O(5) = 3.499(4) Å, C(12)···O(3) = 3.447(3) Å and intra C(8)···O(2) = 3.016(3) Å] in the crystal. Moreover, the centroid–centroid distance of 3.549 Å between the parallel benzotriazole rings of adjacent chains, indicates significant intermolecular face-to-face π-stacking interactions, which further link polymeric chains together with H-bonds to form layer-like supermolecules and stabilize the structure.

Crystal structure of complex 4. In a similar fashion, complex **4**, formed through the combination of $\mathbf{L^1}$ with $CuCl_2$, is also

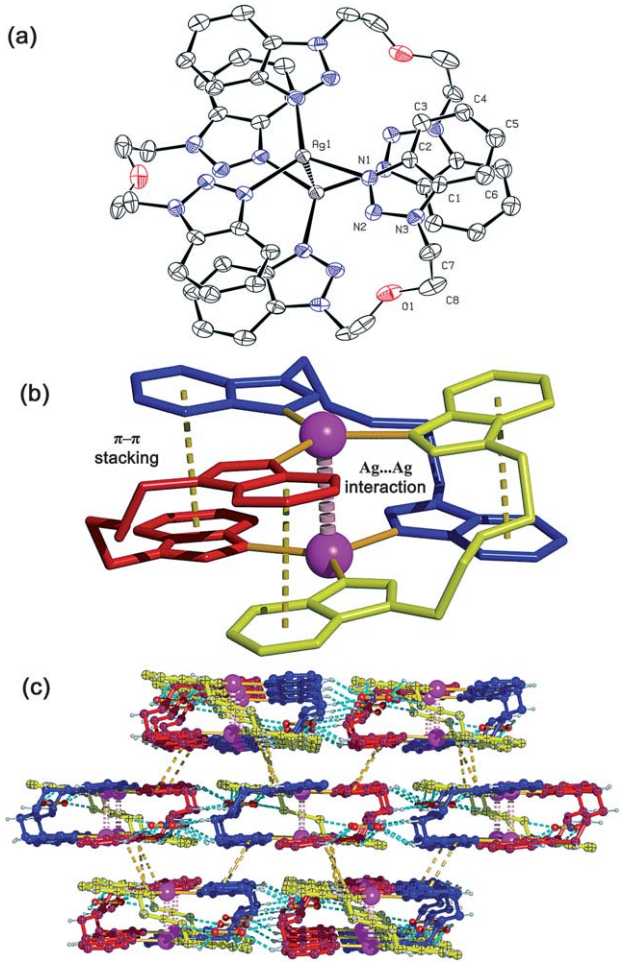

Fig. 2 (a) An ORTEP diagram showing the dinuclear cations of **2** (30% probability ellipsoids). Hydrogen atoms are omitted for clarity. (b) View of Ag···Ag interaction and π–π stacking interactions in the dinuclear unit. (c) The aggregation of the dinuclear cations and the filling of nitrate groups in the packing. Hydrogen bonds are denoted by the turquoise broken line; Ag···Ag interaction and π–π stacking interactions are indicated by the lavender and orange broken lines, respectively.

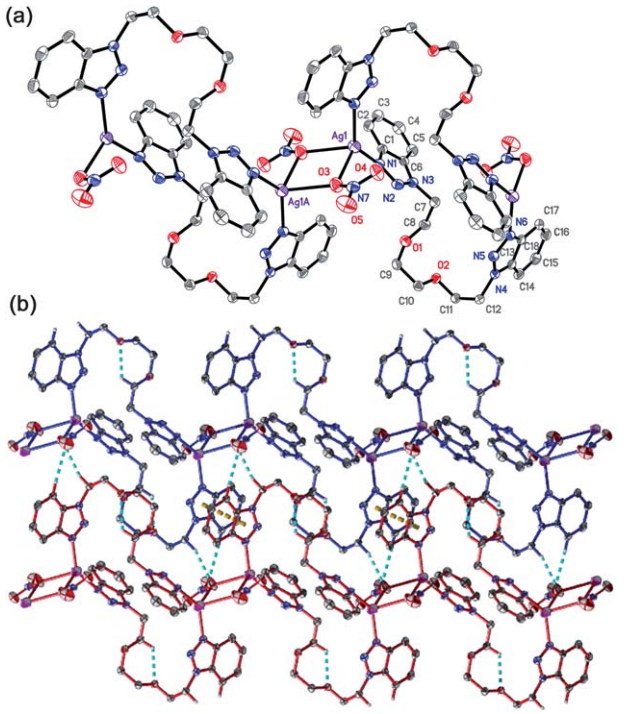

Fig. 3 (a) An ORTEP diagram showing the polymeric chain of **3** (20% probability ellipsoids). Hydrogen atoms are omitted for clarity. Symmetry code: (A) $-1-x, 2-y, 2-z$. (b) 2D layer-like supermolecules formed by aggregations of polymeric chains *via* weak intermolecular hydrogen bonds and π–π stacking interactions. Hydrogen bonds are denoted by the turquoise broken line; π–π stacking interactions are indicated by the orange broken line.

a neutral 1D non-linear coordination polymeric chain running along the crystallographic *b* axis like complex **1**. The crystals suitable for X-ray crystallography conform to the space group $P\bar{1}$; an ORTEP diagram of **4** is shown in Fig. 4a. The Cu^{II} center resides in a distorted *trans*-square planar coordination sphere, which consists of two benzotriazole N-donors and two chlorine atoms.[11n] The *cis*-angles of all ligands around the metal ion are in the range of 90.85°–93.18° and the *trans*-angles are 156.24(6)° and 158.19(13)° respectively. The deviation of Cu^{II} atom from the N2–Cl2 mean plane is equal to 0.04 Å. However, it is worthwhile to note here that in comparison with the structure of complex **1**, the difference of the coordinated anion results in a slight change in the crystal packing. For the V-shaped $\mathbf{L^1}$ with *trans*-conformation, the dihedral angle of two benzotriazole planes is 28.61°, which is 9.15° smaller than that in complex **1**. As indicated in Fig. 4b, two side-by-side chains related by inversion centers close to each other are linked firstly by hydrogen bonding C–H···N [C(8)···N(5) = 3.347(5) Å] forming a 1D polymeric ribbon architecture, which is not found in complex **1**. Then, these 1D polymeric ribbons are further connected by weak hydrogen bonding C–H···Cl [C(7)···Cl(1) = 3.716(4) Å] and two sets of interchain π–π interactions between the benzotriazole-groups (face-to-face distances are 3.68 and 3.80 Å) forming a three-dimensional architecture.

Crystal structure of complex 5. The crystal structure of **5** consists of isolated dinuclear molecules with two bridging chloro ligands. The geometry at each five-coordination Cu^{II} centre is triangle bipyramidal with the basal plane comprising of a terminal chlorine and two bridging chlorine atoms; the apical positions are occupied by the two nitrogen atoms from two bridging ligands, Fig. 5a. The bridging $Cu(\mu\text{–}Cl(1))_2Cu$ unit is strictly planar with a 4-membered ring, with a crystallographically imposed inversion centre in the middle of the dinuclear unit. The distance of the out-of-ring Cu–Cl(2) is 2.2744(8) Å, but the in-ring Cu–(μ–Cl(1)) distances are within the normal range of 2.3784(7) and 2.5332(7) Å respectively, which are slightly longer for the bridging chlorine as expected. In addition, the separated Cu···Cu distance is 3.469 Å and the angles for the 4-membered ring are almost orthogonal [90.20(2)° and 89.80(2)°]. As shown in Fig. 5b, two benzotriazole groups of $\mathbf{L^2}$ in fold mode are approximately parallel to each other with the angle between them being 13.1°. There appear to be intra-dimer stacking interactions on the two sides of the molecule; the shortest distance between benzotriazole planes is 3.83 Å. Moreover, there is a set of

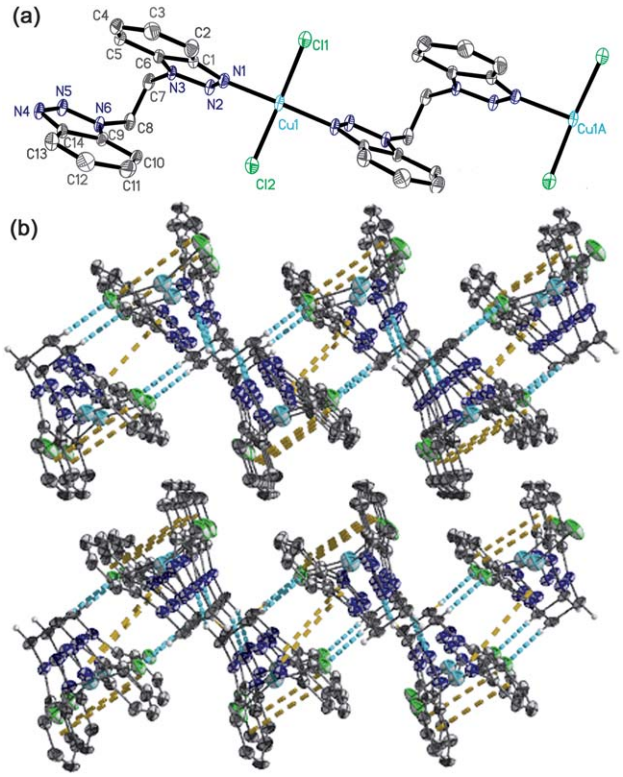

Fig. 4 (a) ORTEP drawing showing the molecular structure of **4** (30% probability ellipsoids). Hydrogen atoms are omitted for clarity. Symmetry code: (A) x, $1 + y$, z. (b) Aggregations of alternate 1D chains link each other through a series of hydrogen bonds and π–π stacking interactions. Hydrogen bonds are denoted by the turquoise broken line; π–π stacking interactions are indicated by the orange broken line.

hydrogen bonds C(15)–H(15)···Cl(1) [C(15)···Cl(1) = 3.405(3) Å] in the molecule to stabilize the structure. In the intermolecular packing, these dimer units are closely stacked together by π–π interactions (3.67 Å and 3.85 Å) and a series of hydrogen bonds, C(7)–H(7B)···O(1) [C(7)···O(1) = 3.524(4) Å], C(10)–H(10B)···N(5) [C(10)···N(5) = 3.423(4) Å] and C(14)–H(14)···Cl(1) [C(14)···Cl(1) = 3.676(4) Å].

Crystal structure of complex 6. The reaction of $CuCl_2$ with $\mathbf{L^3}$ leads to the formation of a neutral bimetallic ring $[Cu_2(\mathbf{L^3})_2Cl_4(DMF)_2]$, in which two ligands act as the organic clips to bridge two metal atoms forming a 30-membered macrometallacycle with a Cu···Cu separation of *ca.* 8.973 Å. As shown in Fig. 6a, two ligands are nearly related by a mirror plane located through two crystallographically independent Cu^{II} atoms and four chlorine atoms. In the dinuclear unit, each Cu^{II} center is bound to two chlorine atoms and an O donor from a DMF molecule to form the basal plane; two coordinated N atoms of $\mathbf{L^3}$ are located at the two apical positions of the axis. Thus, both Cu^{II} centers adopt a five-coordination and the coordination spheres could be described as having a slightly distorted triangle bipyramid geometry, in which the axial Cu–N bonds are significantly shorter than those in the basal plane. In addition, two coordinated DMF molecules are located inside and outside the macrocycle with stronger Cu–O interactions [Cu(1)–O(5) = 2.090(7)

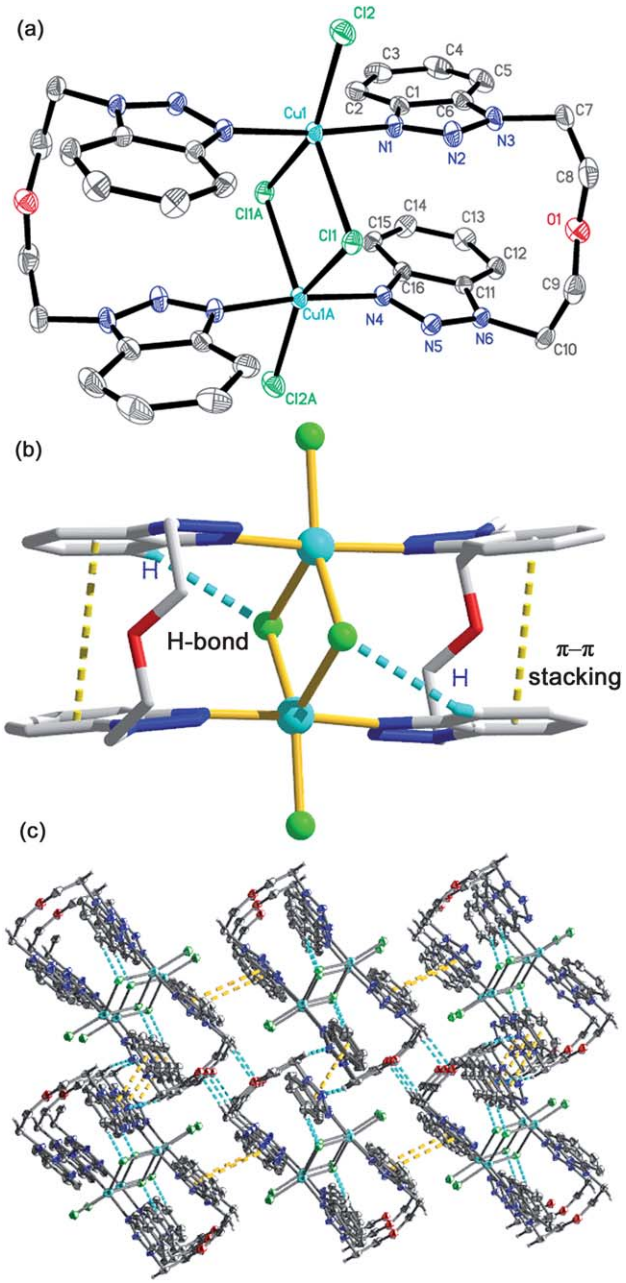

Fig. 5 (a) An ORTEP diagram showing dinuclear structure of **5** (30% probability ellipsoids). Hydrogen atoms are omitted for clarity. Symmetry code: (A) $2 - x$, $-y$, $-z$. (b) View of intramolecular hydrogen bonds and π–π stacking interactions in the dimer unit. (c) Aggregations of dimer units through weak intermolecular hydrogen bonds and π–π stacking interactions. Hydrogen bonds are denoted by the turquoise broken line; π–π stacking interactions are indicated by the orange broken line.

Å and Cu(2)–O(6) = 2.340(6)Å]. Similarly to the previous complexes, there are also many extensive weak hydrogen bonding systems, C–H···Cl [C(7)···Cl(2) = 3.523(8) Å, C(25)···Cl(2) = 3.562(7) Å, C(11)···Cl(3) = 3.538(10) Å, C(29)···Cl(3) = 3.560(8) Å and C(30)···Cl(4) = 3.667(7) Å] and C–H···O [C(12)···O(2) = 3.500(11) Å]. Moreover, a series of the centroid–centroid distances [3.668(5) Å, 3.840(4) Å, 3.785(5) Å and

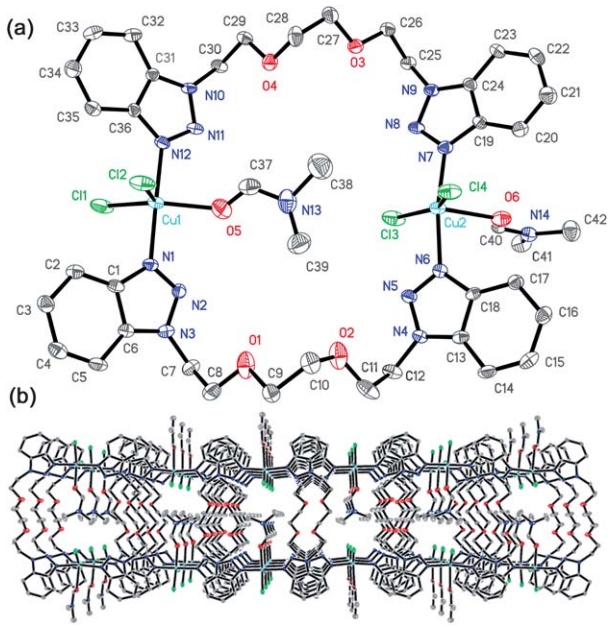

Fig. 6 (a) An ORTEP diagram showing the 30-membered bimetallic ring of **6** (30% probability ellipsoids). Hydrogen atoms are omitted for clarity. (b) 2D layer formed by weak hydrogen bonds and intermolecular π–π aromatic stacking interactions in **6**.

3.722(5) Å] between the parallel benzotriazole rings of adjacent ligands indicates significant intramolecular face-to-face π-stacking interactions, Fig. 6b. Therefore, the thick layered structure is linked and stabilized by these interactions.

Structural comparison of complexes 1–6 and the influencing factors

For three structurally related ligands, each of them has a number of changes in the conformation due to the relative orientations of two terminal groups and the flexible spacer. In these metal complexes, ligands are mainly divided into two types, the same direction (*cis*-) and the opposite direction (*trans*-), according to the difference in the relative orientations of two benzotriazole rings in the ligand without taking into account the shape of the bridging spacer (Scheme 2). As a bridging spacer, the length directly influences the flexibility and the shape of the ligand. In complexes **1** and **4**, ligand $\mathbf{L^1}$ is folded incompletely and takes on a V-shape with *trans*-conformation because of the short spacer. Ligand $\mathbf{L^2}$ with the longer spacer is folded completely and takes on a U-shape with *trans*-conformation for **2** but *cis*-conformation for **5**, and the dihedral angle of the two benzotriazole planes are 0.65° and 13.85°, respectively. With the increasing length of the ligand spacer, the shape of ligand $\mathbf{L^3}$ becomes curved and the type of ligand is more uncertain. The corresponding torsion angles can be found in Tables S1–S6 (ESI†).

For two groups of complexes containing the same metal ions reported in this work, X-ray diffraction studies reveal that they can be classified into three kinds of typical structure featuring mostly 0D dinuclear units for **2** and **5**,1D non-linear coordination polymeric chains for **1** and **4**, and a relatively stable dinuclear metallomacrocycle skeleton for **3** and **6**.

As shown in Scheme 3, it is clearly demonstrated that choosing suitable flexible chain organic ligands is crucial for the formation of complexes with special structures. For ligand $\mathbf{L^1}$ with a shorter spacer, it could not change the configuration easily due to a relatively rigid skeleton structure and can only act as a bridge connecting the adjacent coordination groups of benzotriazoles, resulting in the formation of the similar 1D non-linear coordination polymeric chain for different metal ions. Fortunately, the 1D non-linear chain constructed by 1,2-bis(benzotriazol-1-yl)ethane under mild conditions has not yet been found and is quite different from previously reported using $AgNO_3$ or those metal complexes of $\mathbf{L^1}$ despite the same ligand structure.[3f,11d,j,k] The variety is mostly due to different preparation conditions or the solvent systems for complexes crystal growth.

In **2** and **5**, the spacer of ligand $\mathbf{L^2}$ is longer and the flexibility is enhanced remarkably compared with ligand $\mathbf{L^1}$, which not only leads to ligand molecules adopting multi-bridge modes to connect two metal ions, but the two metal ions are closer to each other to a greater extent to form a dinuclear unit. For ligand $\mathbf{L^3}$ with the longest spacer and most flexible structure, it could not encircle a metal ion to form a 1 : 1 mode complex owing to the disturbance of anion and the limit of chain length. Therefore, it is relatively easy to form the 2 : 2 mode dinuclear metallomacrocycle for **3** and **6** through the connectivity of two ligand bridges. The difference is that there are two nitrate anions to link dinuclear building blocks to self-assemble a 1D chain for **3** but not for **6**. The progressive variation from the 1D non-linear coordination polymeric chain (**1** and **4**) to 0D dinuclear units (**2** and **5**) to a stable dinuclear metallomacrocycle skeleton is mainly

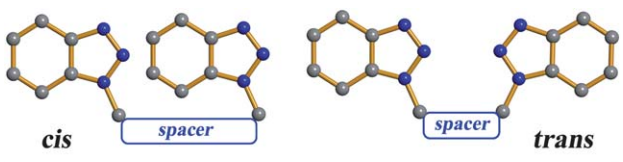

	$\mathbf{L^1}$		$\mathbf{L^2}$		$\mathbf{L^3}$	
Complex	**1**	**4**	**2**	**5**	**3**	**6**
Shape of spacer	**V**		**U**		**S**	**W**
Type of ligand	***trans***		***trans***	***cis***	***cis***	***trans***

Scheme 2 Types and shapes of ligands in the metal complexes.

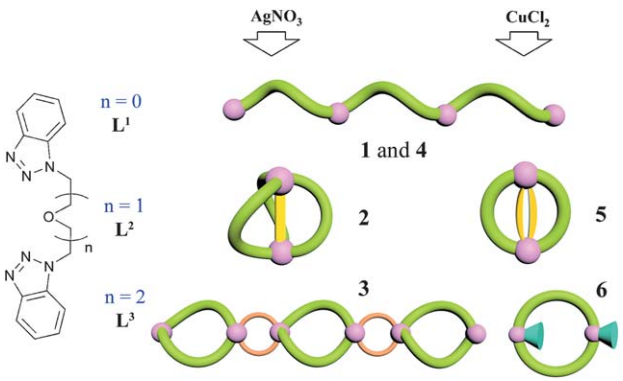

Scheme 3 Schematic view of six complexes in this work.

attributed to the change of the flexible ligand spacers. In other words, the structural diversity and the dimensional change of these complexes are effectively controlled by choosing suitable flexible chain organic ligands.

Thermal analysis

To evaluate the contribution of the correlative flexible ligands with different chain spacer to the thermal stability of complexes with low-dimensional structural features, thermal gravimetric analyses (TGA) of complexes **1–6** were carried out under a nitrogen atmosphere with a heating rate of 10 °C min^{-1} (Fig. 7). For Ag complex **1**, the first weight loss of 6.0% observed from 100 to 125 °C is related to the decomposition of the coordinated acetonitrile molecules (calcd 5.7%). Then, the complex remains largely unchanged until the decomposition of the whole coordination network occurs at the temperature of 262 °C. The TGA of **2** shows that the whole complex structure is stable up to 255 °C. For Ag complex **3**, the weight loss curves also indicate that the frameworks do not collapse until 234 °C. The results reveal clearly that the length of the flexible chain ligand greatly affects the structure and stability of the complex framework, and the decomposition temperature of the complexes gradually increases with progressive structural variation from the flexible metallomacrocycle skeleton (**3**), to 0D dinuclear units (**2**) to 1D coordination polymeric chain (**1**). In other words, the complexes formed by ligands with shorter spacer are more stable than those with longer spacer ligands. In addition, the TGA curves of Cu complexes **4–6** indicate that the decomposition degree of the 1D coordination polymeric chain (**4**) is higher than that of the 0D dinuclear units (**5** and **6**), which are stable up to 290, 254 and 209 °C, respectively. The results also suggest that the complexes with multidimensional structure formed by shorter spacer ligands are more thermally stable, which is similar to Ag complexes **1–3**.

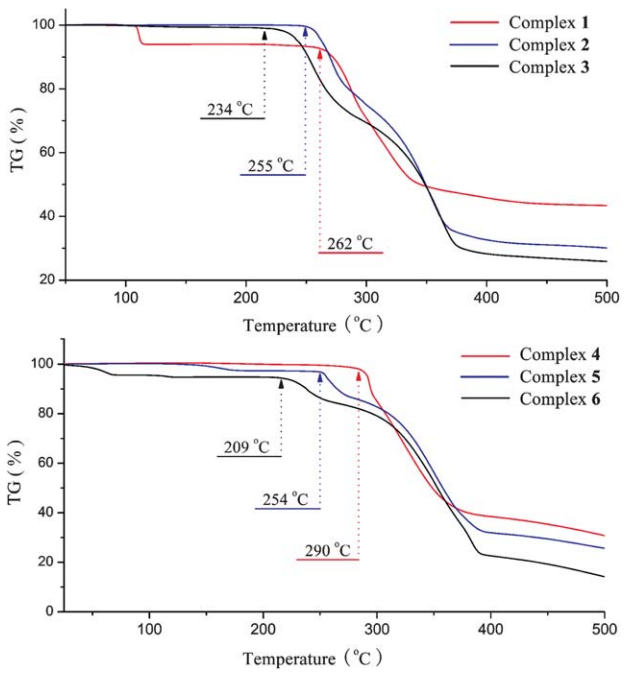

Fig. 7 The TGA curves for complexes **1–6**.

Conclusions

We have designed three structurally related flexible bis(benzotriazole) ligands, and illustrated some useful results of ligand design for self-assembly of diverse coordination aggregates with Ag^{I} and Cu^{II} ions. Without the influence of counteranions, the work clearly indicates that the length of flexible ligand spacers plays an important role in influencing the formation of the coordination architectures. For flexible chain ligands $\mathbf{L^2}$ and $\mathbf{L^3}$ with longer spacers, all complexes are self-assembled to form different dinuclear units, among which **3** is further linked by anions to form an extended 1D chain. But for $\mathbf{L^1}$ with a short spacer, **1** and **4** show similar 1D non-linear coordination polymeric chains despite having different metal centers and different stacking modes. Moreover, the introduction of oxygen atoms in flexible chains could form a series of weak hydrogen bonds, which may provide an effective method for controlling the crystal structures of complexes. The studies on TGA of complexes reveal that the length of flexible chain ligands greatly affects the stability of the complex framework, and the decomposition temperature of complexes gradually increases with progressive structural variation from the flexible metallomacrocycle skeleton, to 0D dinuclear units to 1D non-linear coordination polymeric chains. Accordingly, we believe that further investigation on flexible ligands and understanding various weak interactions will allow a more efficient control of the three-dimensional structure of supramolecular compounds with suitable thermal stability and extend a wide variety of metallosupramolecular architectures.

Acknowledgements

This work was financially supported by the National Natural Science Foundation of China (Grants 20771048, 20931003, 21001059) and the Fundamental Research Funds for the Central Universities (lzujbky-2009-k06, lzujbky-2009-114).

References

1 (*a*) R. Robson, in *Comprehensive Supramolecular Chemistry*, ed. J. L. Atwood, J. E. D. Davies, D. D. MacNicol, F. Vögtle and J. M. Lehn, Pergamon, Oxford, UK, 1996, vol. 6, pp. 733; (*b*) E. R. T. Tiekink and J. J. Vittal, *Frontiers in Crystal Engineering*, John Wiley & Sons, Ltd., England, 2006; (*c*) D. Braga, F. Grepioni and G. R. Desiraju, *Chem. Rev.*, 1998, **98**, 1375; (*d*) P. J. Hagrman, D. Hagrman and J. Zubieta, *Angew. Chem., Int. Ed.*, 1999, **38**, 2638; (*e*) M. Eddaoudi, D. B. Moler, H. L. Li, B. L. Chen, T. M. Reineke, M. O'Keeffe and O. M. Yaghi, *Acc. Chem. Res.*, 2001, **34**, 319; (*f*) A. K. Ghosh, D. Ghoshal, T.-H. Lu, G. Mostafa and N. R. Chaudhuri, *Cryst. Growth Des.*, 2004, **4**, 851; (*g*) S. Kitagawa, R. Kitaura and S. I. Noro, *Angew. Chem., Int. Ed.*, 2004, **43**, 2334.

2 (*a*) R. Robson, B. F. Abrahams, S. R. Batten, R. W. Gable, B. F. Hoskins and J. Liu, in *Supramolecular Architecture*, ed. T. Bein, ACS, Washington, DC, 1992, ch. 19, pp. 256; (*b*) M. Fujita and K. Ogura, *Coord. Chem. Rev.*, 1996, **148**, 249; (*c*) H. Gudbjartson, K. Biradha, K. M. Poirier and M. J. Zaworotko, *J. Am. Chem. Soc.*, 1999, **121**, 2599; (*d*) R. Robson, *J. Chem. Soc., Dalton Trans.*, 2000, 3735; (*e*) S. I. Noro, R. Kitauta, M. Kondo, S. Kitagawa, T. Ishii, H. Matauzaka and M. Yamashita, *J. Am. Chem. Soc.*, 2002, **124**, 2568; (*f*) L. Carlucci, G. Ciani, D. M. Proserpio and L. Spadacini, *CrystEngComm*, 2004, **6**, 96; (*g*) J.-P. Zhang, Y.-Y. Lin, X.-C. Huang and X.-M. Chen, *Chem. Commun.*, 2005, 1258; (*h*) M. Ikeda, Y. Tanaka, T. Hasegawa, Y. Furusho and E. Yashima, *J. Am. Chem. Soc.*, 2006, **128**, 6806; (*i*) H.-C. Chen, H.-L. Hu, Z.-K. Chan, C.-W. Yeh, H.-W. Jia, C.-

P. Wu, J.-D. Chen and J.-C. Wang, *Cryst. Growth Des.*, 2007, **7**, 698; (*j*) H.-J. Kim, E. Lee, M. G. Kim, M.-C. Kim, M. Lee and E. Sim, *Chem.–Eur. J.*, 2008, **14**, 3883.

3 For examples: (*a*) C. Y. Su, Y. P. Cai, C. L. Chen, F. Lissner, B. S. Kang and W. Kaim, *Angew. Chem., Int. Ed.*, 2002, **41**, 3371; (*b*) S. Masaoka, D. Tanaka, Y. Nakanishi and S. Kitagawa, *Angew. Chem., Int. Ed.*, 2004, **43**, 2530; (*c*) Y. T. Wang, H. H. Fan, H. Z. Wang and X. M. Chen, *Inorg. Chem.*, 2005, **44**, 4148; (*d*) X.-C. Huang, D. Li and X.-M. Chen, *CrystEngComm*, 2006, **8**, 351; (*e*) C.-Y. Lin, Z.-K. Chan, C.-W. Yeh, C.-J. Wu, J.-D. Chen and J.-C. Wang, *CrystEngComm*, 2006, **8**, 841; (*f*) J. Zhou, X. Liu, Y. Zhang, B. Li and Y. Zhang, *Inorg. Chem. Commun.*, 2006, **9**, 216; (*g*) X. Zhang, X.-P. Zhou and D. Li, *Cryst. Growth Des.*, 2006, **6**, 1440; (*h*) M. O. Awaleh, A. Badia and F. Brisse, *Cryst. Growth Des.*, 2006, **6**, 2674; (*i*) S. T. Wu, L. S. Long, R. B. Huang and L. S. Zheng, *Cryst. Growth Des.*, 2007, **7**, 1746; (*j*) B. Zheng, H. Dong, J. Bai, Y. Li, S. Li and M. Scheer, *J. Am. Chem. Soc.*, 2008, **130**, 7778; (*k*) R. Peng, S.-R. Deng, M. Li, D. Li and Z.-Y. Li, *CrystEngComm*, 2008, **10**, 590; (*l*) J. Liang, B. Wu, C. Jia and X. Yang, *CrystEngComm*, 2009, **11**, 975.

4 For examples: (*a*) S. X. Liu, S. Lin, B. Z. Lin, C. C. Lin and J. Q. Huang, *Angew. Chem., Int. Ed.*, 2001, **40**, 1084; (*b*) S. Banfi, L. Carlucci, E. Caruso, G. Ciani and D. M. Proserpio, *J. Chem. Soc., Dalton Trans.*, 2002, 2714; (*c*) J. R. Li, R. H. Zhang and X. H. Bu, *Cryst. Growth Des.*, 2003, **3**, 829; (*d*) C. L. Chen, C. Y. Su, Y. P. Cai, H. X. Zhang, A. W. Xu and B. S. Kang, *Inorg. Chem.*, 2003, **42**, 3738; (*e*) X. L. Wang, C. Qin and E. B. Wang, *Angew. Chem., Int. Ed.*, 2004, **43**, 5036; (*f*) Y. F. Peng, H. Y. Ge, B. Z. Li, B. L. Li and Y. Zhang, *Cryst. Growth Des.*, 2006, **6**, 994; (*g*) B. L. Li, X. Y. Wang, X. Zhu, S. Gao and Y. Zhang, *Polyhedron*, 2007, **26**, 5219; (*h*) L. Y. Wang, Y. Yang, K. Liu, B. L. Li and Y. Zhang, *Cryst. Growth Des.*, 2008, **8**, 3902.

5 (*a*) S. Leininger, B. Olenyuk and P. J. Stang, *Chem. Rev.*, 2000, **100**, 853; (*b*) S. M.-F. Lo, S. S.-Y. Chui, L. Y. Shek, Z. Lin, X. X. Zhang, G. Wen and I. D. Williams, *J. Am. Chem. Soc.*, 2000, **122**, 6293; (*c*) B. Moulton and M. J. Zaworotko, *Chem. Rev.*, 2001, **101**, 1629; (*d*) M. Fujita, K. Umemoto, M. Yoshizawa, N. Fujita, T. Kusukawa and K. Biradha, *Chem. Commun.*, 2001, 509; (*e*) M. Eddaoudi, J. Kim, N. Rosi, D. Vodak, J. Wachter, M. O'Keeffe and O. M. Yaghi, *Science*, 2002, **295**, 469; (*f*) K. Barthelet, J. Marrot, D. Riou and G. Férey, *Angew. Chem., Int. Ed.*, 2002, **41**, 281; (*g*) T. Kusukawa and M. Fujita, *J. Am. Chem. Soc.*, 2002, **124**, 13576; (*h*) J. Luo, M. Hong, R. Wang, R. Cao, L. Han, Z. Lin and Y. Zhou, *Inorg. Chem.*, 2003, **42**, 4486; (*i*) B.-H. Ye, M.-L. Tong and X.-M. Chen, *Coord. Chem. Rev.*, 2005, **249**, 545; (*j*) H. M. El-Kaderi, J. R. Hunt, J. L. Mendoza-Cortés, A. P. Côté, R. E. Taylor, M. O'Keeffe and O. M. Yaghi, *Science*, 2007, **316**, 268; (*k*) S. Ma, X.-S. Wang, C. D. Collier, E. S. Manis and H.-C. Zhou, *Inorg. Chem.*, 2007, **46**, 8499; (*l*) J.-J. Wang, C.-S. Liu, T.-L. Hu, Z. Chang, C.-Y. Li, L.-F. Yan, P.-Q. Chen, X.-H. Bu, Q. Wu, L.-J. Zhao, Z. Wang and X.-Z. Zhang, *CrystEngComm*, 2008, **10**, 681; (*m*) C.-S. Liu, J.-J. Wang, Z. Chang, L.-F. Yan and X.-H. Bu, *CrystEngComm*, 2010, **12**, 1833.

6 (*a*) L. Carlucci, G. Ciani, D. M. Proserpio and S. Rizzato, *CrystEngComm*, 2002, **4**, 413; (*b*) X.-H. Bu, W. Chen, W.-F. Hou, M. Du, R.-H. Zhang and F. Brisse, *Inorg. Chem.*, 2002, **41**, 3477; (*c*) Y.-B. Xie, C. Zhang, J.-R. Li and X.-H. Bu, *Dalton Trans.*, 2004, 562; (*d*) G. H. Cui, J. R. Li, J. L. Tian, X. H. Bu and S. R. Batten, *Cryst. Growth Des.*, 2005, **5**, 1775.

7 (*a*) L. Raehm, L. Mimassi, C. Guyard-Duhayon and H. Amouri, *Inorg. Chem.*, 2003, **42**, 5654; (*b*) B. Chatterjee, J. C. Noveron, M. J. E. Resendiz, J. Liu, T. Yamamoto, D. Parker, M. Cinke, C.; (*c*) V. Nguyen, A. M. Arif and P. J. Stang, *J. Am. Chem. Soc.*, 2004, **126**, 10654; (*d*) N. L. S. Yue, M. C. Jennings and R. J. Puddephatt, *Inorg. Chem.*, 2005, **44**, 1125; (*e*) C. L. Chen, H. Y. Tan, J. H. Yao, Y. Q. Wan and C. Y. Su, *Inorg. Chem.*, 2005, **44**, 8510.

8 (*a*) G. H. Cui, J. R. Li, J. L. Tian, X. H. Bu and S. R. Batten, *Cryst. Growth Des.*, 2005, **5**, 1775; (*b*) C. M. Jin, H. Lu, L. Y. Wu and J. Huang, *Chem. Commun.*, 2006, 5039; (*c*) X. J. Li, X. Y. Wang, S. Gao and R. Gao, *Inorg. Chem.*, 2006, **45**, 1508; (*d*) L. L. Wen, Z. D. Liu, J. G. Lin, Z. F. Tian, H. Z. Zhu and Q. J. Meng, *Cryst. Growth Des.*, 2007, **7**, 93; (*e*) Y. Y. Liu, J. F. Ma, J. Yang and Z. M. Su, *Inorg. Chem.*, 2007, **46**, 3027; (*f*) Y. Qi, Y. Che, F. Luo, S. R. Batten, Y. Liu and J. Zheng, *Cryst. Growth Des.*, 2008, **8**, 1654.

9 (*a*) G. F. Kokoszka, J. Baranowski, C. Goldstein, J. Orsini, A. D. Mighell, V. L. Himes and A. R. Siedle, *J. Am. Chem. Soc.*, 1983, **105**, 5627; (*b*) A. R. Katritzky, X. Lan, J. Z. Yang and O. V. Denisko, *Chem. Rev.*, 1998, **98**, 409.

10 (*a*) D. S. Moore and S. D. Robinson, *Adv. Inorg. Chem.*, 1988, **32**, 171; (*b*) M. Murrie, D. Collison, C. D. Garner, M. Helliwell, P. A. Tasker and S. S. Turner, *Polyhedron*, 1998, **17**, 3031.

11 (*a*) B. J. O'Keefe and P. J. Steel, *Inorg. Chem. Commun.*, 2000, **3**, 473; (*b*) H. Hou, X. Meng, Y. Song, Y. Fan, Y. Zhu, H. Lu, C. Du and W. Shao, *Inorg. Chem.*, 2002, **41**, 4068; (*c*) X. Meng, Y. Song, H. Hou, Y. Fan, G. Li and Y. Zhu, *Inorg. Chem.*, 2003, **42**, 1306; (*d*) J. Zhou, Y. Peng, Y. Zhang, B. Li and Y. Zhang, *Inorg. Chem. Commun.*, 2004, **7**, 1181; (*e*) P. Børsting and P. J. Steel, *Eur. J. Inorg. Chem.*, 2004, 376; (*f*) L. F. Jones, L. O'Dea, D. A. Offermann, P. Jensen, B. Moubaraki and K. S. Murray, *Polyhedron*, 2006, **25**, 360; (*g*) J. Zhou, X. Liu, Y. Zhang, B. Li and Y. Zhang, *Inorg. Chem. Commun.*, 2006, **9**, 216; (*h*) X. Zhou, X. Meng, W. Cheng, H. Hou, M. Tang and Y. Fan, *Inorg. Chim. Acta*, 2007, **360**, 3467; (*i*) X. Meng, J. Li, H. Hou, Y. Song, Y. Fan and Y. Zhu, *J. Mol. Struct.*, 2008, **891**, 305; (*j*) M.-C. Hu, Y. Wang, Q.-G. Zhai, S.-N. Li, Y.-C. Jiang and Y. Zhang, *Inorg. Chem.*, 2009, **48**, 1449; (*k*) Y. Wang, M.-C. Hu, Q.-G. Zhai, S.-N. Li, Y.-C. Jiang and W.-J. Ji, *Inorg. Chem. Commun.*, 2009, **12**, 281; (*l*) L.-L. Li, H.-X. Li, Z.-G. Ren, D. Liu, Y. Chen, Y. Zhang and J.-P. Lang, *Dalton Trans.*, 2009, 8567; (*m*) X. Gao, Q.-G. Zhai, S.-N. Li, R. X., H.-J. Xiang, Y.-C. Jiang and M.-C. Hu, *J. Solid State Chem.*, 2010, **183**, 1150; (*n*) K. Skorda, T. C. Stamatatos, A. P. Vafiadis, A. T. Lithoxoidou, A. Terzis, S. P. Perlepes, J. Mrozinski, C. P. Raptopoulou, J. C. Plakatouras and E. G. Bakalbassis, *Inorg. Chim. Acta*, 2005, **358**, 565.

12 (*a*) X. Tang, W. Dou, S. Chen, F. Dang and W. Liu, *Spectrochim. Acta, Part A*, 2007, **68**, 349; (*b*) J. Mao, L. N. Wang, W. Dou, X. L. Tang, Y. Yan and W. S. Liu, *Org. Lett.*, 2007, **9**, 4567; (*c*) X. Song, W. Liu, W. Dou, Y. Wang, J. Zheng and Z. Zang, *Eur. J. Inorg. Chem.*, 2008, 1901; (*d*) X. Song, W. Liu, W. Dou, J. Zheng, X. Tang, H. Zhang and D. Wang, *Dalton Trans.*, 2008, 3582; (*e*) Y. Guo, W. Dou, X. Zhou, W. Liu, W. Qin, Z. Zang, H. Zhang and D. Wang, *Inorg. Chem.*, 2009, **48**, 3581; (*f*) X. Zhou, B. Yu, Y. Guo, X. Tang, H. Zhang and W. Liu, *Inorg. Chem.*, 2010, **49**, 4002.

13 *Bruker, SMART and SAINT*; Bruker AXS Inc.: Madison, Wisconsin, 2004.

14 (*a*) G. M. Sheldrick, *SHELXS-97, Program for Crystal Structure Solution*, University of Göttingen, Göttingen, Germany, 1997; (*b*) G. M. Sheldrick, *SHELXL-97, Program for Crystal Structure Refinement*, University of Göttingen, Göttingen, Germany, 1997.

